Academic Journal of Science and Technology
ISSN: 2771-3032 | Vol. 11, No. 2, 2024

Deformation and Force Analysis of Utility Tunnel joint under Longitudinal Uneven Foundation

Liwen Zhu, Xinsheng Zhang, Jinglong Wu, Ben Li

School of Civil Engineering, Central South University of Forestry and Technology, Changsha 410000, China

Abstract: To study the regularity of force and deformation of utility tunnels under longitudinal uneven foundations, considering the traffic load, the authors established a finite element model based on pipe-soil interaction to analyze the effect of different working conditions on force and deformation of utility tunnel joints. The results indicated that different stiffness of the foundation can lead to different mechanical properties of the utility tunnel top plate, bottom plate and socket joints. The deformation of the bell joint which on the undisturbed soil and located 2 to 3 sections pipes to the replacement junction changes most obviously, meanwhile, as the longitudinal stiffness difference increases, the maximum horizontal opening on the top plate shifts closer to the replacement junction, and the maximum opening up to 3.561mm; the phenomenon of axial stress below the waterproof requirement exists in the interface of the top plate on the undisturbed soil and the interface of the bottom plate on the replacement soil at the difference in stiffness of the foundation is greater; the maximum differential settlement of joint is located the first corridor interface to the replacement junction which on the undisturbed soil, that is characterized by 'decreasing from the replacement junction to both sides'.

Keywords: Utility Tunnel; Socket Joint; Differential Settlement; Foundation Stiffness; Numerical Analysis.

1. Introduction

Underground comprehensive utility tunnel, as a shallow-buried underground framework structure, has strict requirements for the foundation soil. When the utility tunnel route needs to pass through soft and weak soil layers, the replacement method is usually adopted to improve the foundation soil (Xie, 2021). In special sections, such as the transition region from loose to dense soil layers when using replacement methods, varying degrees of subsidence may occur under external loads due to differences in the physical and mechanical properties of the soil. If foundation differential settlement is not properly controlled, it will lead to cracking and damage of the utility tunnel structure, especially at the joints where relative angles may cause joint opening, up-down mismatch and water leakage issues (Li, 2022 & Yi, 2017). Especially seepage at tunnel could intensify settlement deformation (Li, 2022). Therefore, it is necessary to study the influence of soil layer heterogeneity on the utility tunnel, and analyse its mechanical characteristics, especially for areas where there are significant changes in the foundation soil.

Sonoda (2022) found that the main strain direction in the pipe joint had changed under uneven settlement through model tests. Bai (2018) used finite element software to carry out the research from the perspective of the influence law of uneven settlement on the crack width between sections of the utility tunnel. The results revealed that uneven settlement has a large impact on cracks between sections of the utility tunnel, which can lead to damage to connecting bolts and failure of waterproof joints in severe cases. Uneven settlement of foundation soil can lead to structural cracking of underground structures, which in turn affects their performance. At the same time, ground cracks have a significant impact on the structural stability of corridors. Yan (2018) carried out numerical analysis of the impact of ground fissure dislocation on the stress and deformation of underground utility tunnels, and found that the greater the ground fissure dislocation, the greater the tension damage to the top and bottom plates of the corridor structure and the dislocation at the joints. Miao (2022) carried out numerical simulation and theoretical analysis on the impact of shield tunnelling under a site with ground cracks on existing utility tunnel structures, with actual engineering as the background. They found that the effect of ground cracks on the pipe gallery structure was manifested as superposition and amplification of deformation.

Due to the utility tunnels are much larger in longitudinal scale than horizontal, resulting in their relatively weak longitudinal stiffness and are easily affected by many factors such as differences in foundation stiffness. Wei (2013) investigated the impact of soil heterogeneity on vertical settlement in immersed tube tunnels through theoretical calculations and engineering practice. Through a systematic study of settlement data from 20 immersed tunnels, Shao (2013) reached the allowable value of settlement. Through the analysis of extensive settlement data from immersed tube tunnels, researchers (Grantz, 2001) have found that the implementation of effective foundation treatment measures can effectively mitigate the effects of differential settlement on the structure of underground tunnels. Consequently, it is partially guiding significant for foundation treatment measures to investigate deformation laws of utility tunnels under different settlements. Nevertheless, much of the existing research has focused on the local damage mechanisms of corridor joints, the deformation characteristics of the overall corridor structure under longitudinal non-uniformity of the fill foundation are still unclear, and the research findings in this area are relatively sparse. Therefore, investigating the impact of non-uniform foundations on the force deformation of corridor joints has significant engineering utility.

To provide a reference for the stability of the power corridor during design and construction, this paper combines a municipal corridor project with several typical longitudinal infill foundation conditions, establishes a finite element model, and investigates the law of force deformation of

corridor joints under longitudinal non-uniform foundation conditions.

2. Establishment of Calculate Model

2.1. Geometry and Unit Settings

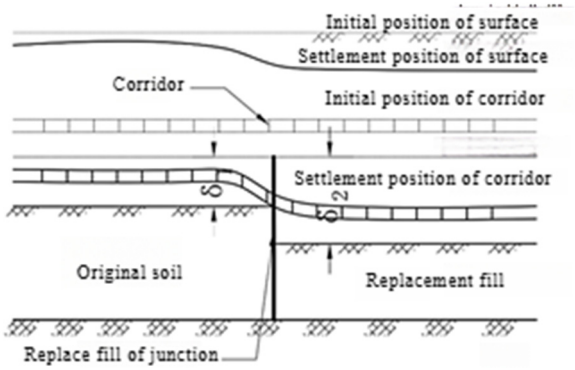

Fig 1. Settlement and deformation model for underground utility tunnel

Based on the theoretical model of foundation differences (Shen, 2010), the author developed a settlement deformation model for a corridor with longitudinal uneven foundation conditions by considering variations in the mechanical properties of different replacement soils, shown in Figure 1. (In figure 1, the settlement of undisturbed soil or rock mass is δ1, the settlement of replacement soil is δ2)

Using ABAQUS finite element simulation software, a 3D solid model of the soil and corridor was established to simulate the entire backfill process during the construction of a utility tunnel project. The model has dimensions of 60.15×36×30 m, consisting of a 20-section vertical prefabricated utility tunnel, with each section measuring 3.15×3.6×3.2 m. The calculation model is shown in Figure 2. The C3D8R unit, an 8-node hexahedral element with linear reduction, is used to model concrete structures, bedding layers, and stranded anchorage ends in underground utility tunnels. Considering the effects of groundwater infiltration and pore water pressure on soil deformation, the C3D8P model is used for soil analysis. The T3D2 unit, a 2-node linear 3D spatial truss element, is used to simulate the built-in reinforcement and prestressing strands of the structural body of the utility tunnel, and the elements are divided by structured meshing, swept meshing and free meshing techniques respectively. The mesh division of model is shown in Figure 3.

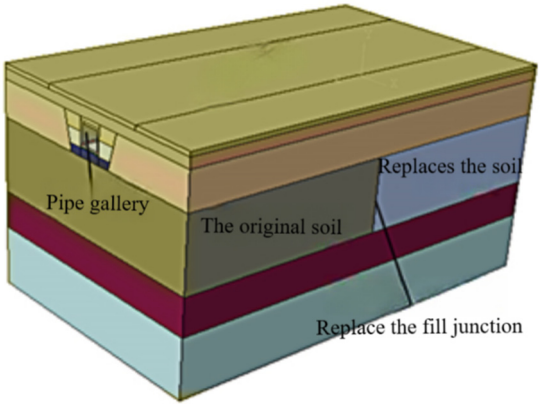

Fig 2. Corridor-soil 3D calculation model

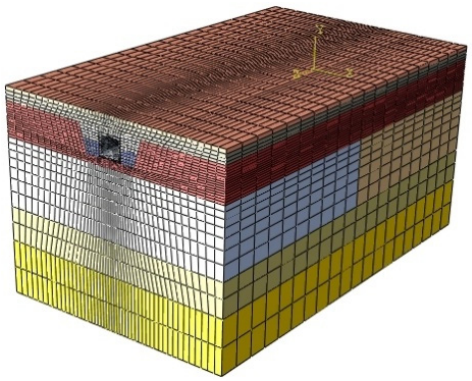

Fig 3. Mesh division of model

2.2. Material Parameters and Contact Property Settings

Interaction between different solid elements adopts “hard contact” in the vertical direction and Coulomb friction contact in the tangential direction. Material parameters for each structural model are shown in Table 1.

Table 1. Mechanical parameters of utility tunnel and soil structure materials

Type of material	Density ρ/ (kg·m^{-3})	Constrained modulus E_s/MPa	Poisson ratio ν	Cohesion c/KPa	Internal friction angel φ/ (°)	Pore ratio e	Permeability coefficient k/(m·d^{-1})
corridor	2500	32 500	0.2	-	-	-	-
Pavement material	2400	1400	0.35	-	-	-	-
Replacement soil	1930	5.8	0.27	25	18	-	0.05
Sand gravel (3:7)	2150	15	0.25	1	35	0.6	0.3
strongly weathered argillaceous limestone	2300	*100	0.30	220.0	35	-	0.009
silty clay	1900	5	0.3	20	14	0.8	0.06
plain soil	1900	20	0.33	135.0	21.0	0.624	0.065
earth-rock mixture	2120	40	0.32	110.0	34.0	0.6	0.3
block stone mixture	2000	80	0.30	57.0	35	0.6	0.1
strong weathered limestone	2400	*150	0.3	356	33	-	0.015
medium weathered limestone	2600	*300	0.26	1000	38	-	0.008

Remark: the data with "*" in front of the data in the table is the empirical data, and the data with "()" in the data is the data obtained by the model calculation, and the conversion relationship between the modulus of elasticity E and the modulus of compression Es is $E=\frac{2(1-\nu^2)}{1-\nu}E_S$.

3. Numerical Analysis Methods

3.1. Foundation Conditions

During the construction process, a small step excavation method is utilized for the inclined bedrock surface along with backfill compaction. There are two primary forms of in situ rock and soil: heavily weathered marl(Y1) and chalky clay(Y2). Due to ongoing construction activities, the soil quality in the backfill area varies greatly, consisting of three primary soil types: plain soil(T1), soil-stone mixture(T2), and stone-lump mixture(T3). Uneven foundation conditions with different soil combinations are shown in the Table 2.

Table 2. Simulated working conditions of different foundations

Soil type		Coding	Foundation type		Coding
In-situ soli	heavily weathered marl	Y1	Replacement foundation Combination design	heavily weathered marl- chalky clay	Y1-Y2
	chalky clay	Y2		heavily weathered marl- plain soil	Y1-T1
Replacement soil	plain soil	T1		heavily weathered marl- soil-stone mixture	Y1-T2
	soil-stone mixture	T2		heavily weathered marl- stone-lump mixture	Y1-T3
	stone-lump mixture	T3			

3.2. Load Simulation

Apart from the self-weight load of the structure, underground power pipe galleries are also subjected to vertical and horizontal soil pressures from the surrounding environment, static water pressure from groundwater, as well as pressures from vehicular traffic, crowds, and localized loading. There was research (Xu, 2019) shown that pipe galleries can undergo significant displacement due to dynamic vehicle loads.

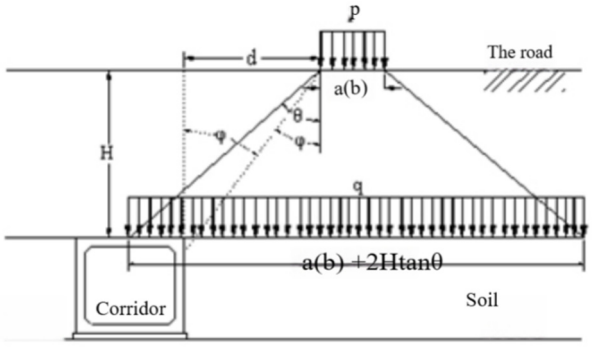

Fig 4. Calculated diagram of equivalent vehicular load

This paper provides a correction value for the top load values of the pipe gallery structure, taking into consideration the influence of vehicle loads on the road surface. The calculated load of element model is shown in the Figure 4.

Considering the fact that there are more heavy vehicles on the road after the backfill and compaction of the construction of the underground utility tunnel, refer to the existing literature (Shi, 2009&Tang,2019) and combine the even load with the dynamic load factor (taken as 0.4), and then obtain an improved even load value on the top of the utility tunnel. The improved load calculation formula is as shown in Equation 1.

$$q=\frac{(1+\mu)\sum p}{(a+2H\tan 30^\circ)(b+2H\tan 30^\circ)} \quad (1)$$

In Equation 1, q' (kPa) is the value of the even load spreading by the improved wheel load to the top of the pipe, μ is the dynamic load factor for the vehicle load, p (kPa) is the wheel pressure, a (m) and b (m) is the length and width of the contact surface between the tyre and the ground, H (m) is the burial depth of pipe.

Vehicle loads impact depth range is generally within 6 to 10 meters (Qiu, 2010), the loading width of uniform constant load on the surface is set as 20 meters, vehicle loads are taken as 300kN, a left and right wheelbase of 1.8 meters and a front and rear wheelbase of 5.4 meters, the dimensions of the contact surface between the front and rear wheels and the ground are respectively 0.3m×0.2m and 0.6m×0.2m. After the conversion of formula (1), the earth surface even load is taken as 20kPa.

4. Analysis of Results

4.1. Axial Stress Analysis

Through extracting axial stresses at the top and bottom mid-span of the utility tunnel at each joint within a longitudinal range of 60 meters, and assuming no change in foundation differences beyond this range, an analysis is conducted to investigate the impact of foundation differences on the stress and deformation of the utility tunnel structure. Under Y1-T1 operational conditions, the axial stress distribution curves for the top and bottom plates at the midspan joint of the corridor, at different backfill heights, are depicted in Figure 5. Additionally, the axial stress cloud diagram for the top and bottom plates is presented in Figure 6.

By comparing Figure 5(a) with Figure 5(b) axial stresses can be observed at the top and bottom midspan of the corridor joint exhibit an ‘S’ shaped distribution along the longitudinal direction with an increase in backfill height. This indicates that under the longitudinal non-uniform foundation differences, axial stresses at the top and bottom midspan of

the corridor at the joint vary as the backfill height increases.

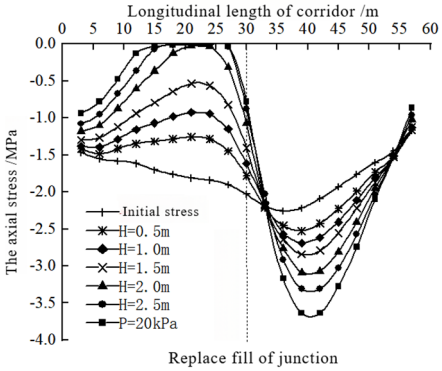

Fig 5a. Axial stress distribution curve at the top plate of pipe gallery joints

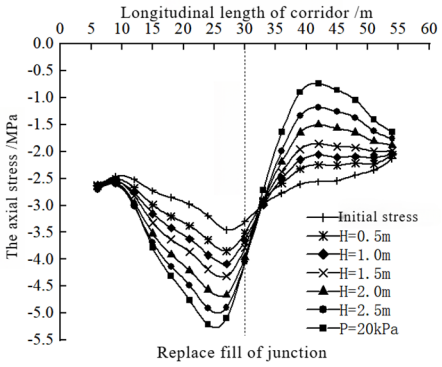

Fig 5b. Axial stress distribution curve at the bottom plate of pipe gallery joints

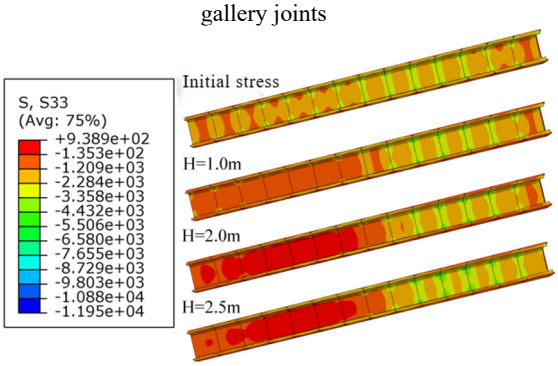

Fig 6a. Axial stress distribution cloud diagram at the top plate of pipe gallery joints

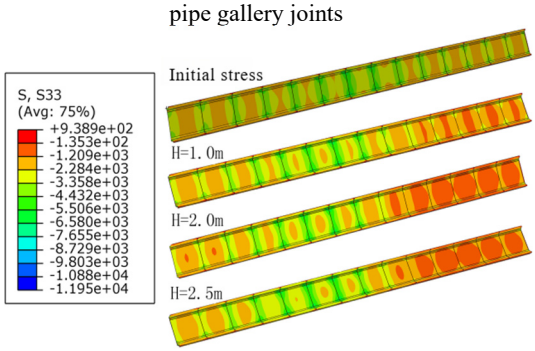

Fig 6b. Axial stress distribution cloud diagram at the bottom plate of pipe gallery joints

In the original soil section, axial stress at the joint of the top plate decreases consistently, while the bottom plate experiences a continuous increase. On the other hand, for the corridor in the replacement foundation section, the axial stress at the joint of the top plate continuously increases, while the bottom plate continuously decreases. The increase in the height of the backfill leads to an augmented vertical soil pressure acting on the corridor. Additionally, the replacement soil typically exhibits high compressibility, resulting in significant vertical displacement of the pipe gallery in the replacement junction, while the original soil section experiences comparatively lesser vertical displacement. Consequently, there is an escalation in the differential longitudinal settlement at the soil replacement junction, resulting in significant variations in axial stresses at the joint of the pipe gallery. The minimum axial stress for the top plate of the pipe gallery located at the in-situ foundation falls below 1.5MPa when the backfill height exceeds 0.5m. Similarly, for the bottom plate of the pipe gallery located at the replacement foundation, the minimum axial stress falls below 1.5MPa when the backfill height exceeds 2.0m. These values fail to meet the waterproofing requirement for the elastic sealing pad stress at the joint, which must not be less than 1.5MPa (Ministry of Housing and Urban-Rural Development of the People's Republic of China, 2015). The stress curves of varying backfill heights depicted in Figure 5 intersect at a point on the right side of the backfill interface, indicating that the axial stress of the gallery's top and bottom plates, which located at one section of gallery to the right of the replacement soil junction, is not influenced by the height of the backfill or the dynamic loading of vehicular traffic on the road surface.

As shown in Figure 6(a) and 6(b), with the increase in fill height, the red area of the top plate and the green area of the bottom plate at the corridor interface on the left side of the replacement junction increase significantly. Conversely, the green area of the top plate and the red area of the bottom plate at the right side of the pipe corridor interface increase significantly. It indicates that with the increase of filling height, the axial stress at the interface of the top plate of the pipe corridor on the left side of the replacement junction keeps decreasing and the axial stress of the bottom plate keeps increasing; the axial stress at the interface of the top plate of the pipe corridor on the right side of the replacement junction keeps increasing and the axial stress of the bottom plate keeps decreasing.

Axial stress distribution curves for the mid-span of the top and bottom plates at the joint in the gallery, subject to different non-uniform longitudinal foundation conditions, are represented in Figure 7, where the backfill height is taken as an example with a value of 2.5m.

As shown in Figure 7, it can be observed that under different combinations of replacement foundations, the greater the differential longitudinal foundation stiffness, the more significant the axial stress variation at the gallery interface at the replacement junction. The axial stress of the top plate of the gallery on undisturbed soil decreases continuously, while that of the bottom plate increases continuously. Conversely, on the side of the cut-and-fill soil, the axial stress of the top plate of the gallery gradually increases, while that of the bottom plate gradually decreases. This phenomenon can be attributed to the stiffness discrepancy of the longitudinal foundation, which results in uneven settlement of the replacement junction foundation under the same loading conditions. Consequently, this

variation causes an obvious change in axial stresses in the gallery structure located at the replacement junction.

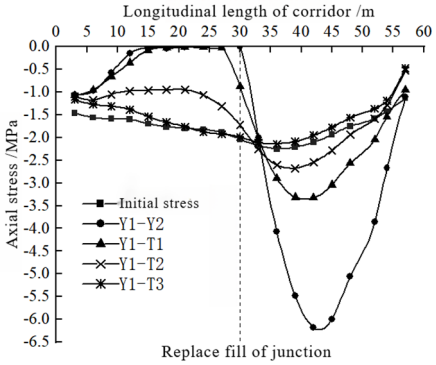

Fig 7a. Axial stress distribution curve at top plate of the joints of pipe gallery

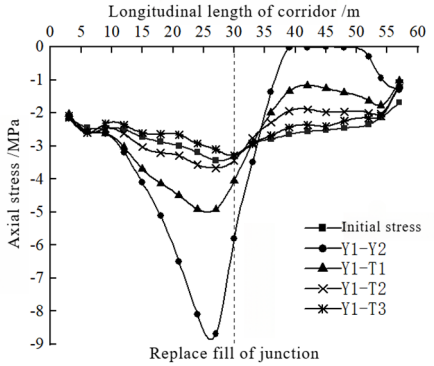

Fig 7b. Axial stress distribution curve at bottom plate of the joints of pipe gallery

Under Y1-Y2 and Y1-T1 working conditions, the minimum axial stress experienced by the top plate on the left and bottom plate on the right side of the replacement junction surface is less than 1.5 MPa. Similarly, under working conditions Y1-T2 and Y1-T3, the minimum axial stress experienced by the top plate on the left side of the replacement junction surface is also less than 1.5 MPa. When the ratio of longitudinal non-uniform foundation stiffness difference (represented by λ) is equal to or greater than 1.25, the interfacial connection of the top plate of the corridor on the left side of the replacement soil junction may not meet the specification for inter-sectional interface stress waterproofing requirement of 1.5 MPa at the joints. Meanwhile, when λ is equal to or greater than 5, the interfacial connection of the bottom plate of the corridor on the right side of the replacement soil junction may not meet the same specification.

Under Y1-Y2 working conditions, axial stresses at the interface between the 1-5 sections of pipes on the left side of the replacement soil junction and the 3-6 sections of pipes on the right side of the replacement soil junction are near zero. This means that there may be a separation of the spigot end and bell joint at the interface, ultimately leading to water leakage in the corridor structure. In addition, the longitudinal foundation difference did not appear to affect axial stresses at the first section of the corridor interface on the right side of the replacement junction.

4.2. Strain Analysis

The strain distribution on the top and bottom plates at the midspan of bell joints and spigot ends at various interfaces of the corridor structure is illustrated in Figure 8.

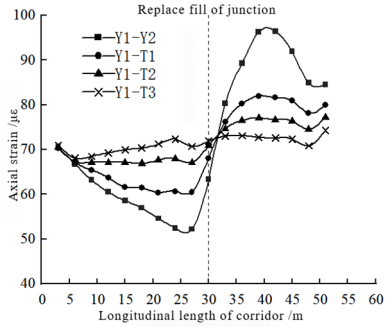

Fig 8a. Midspan strain distribution curve of the top plate at the bell ends

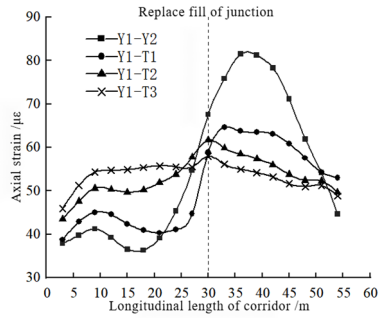

Fig 8b. Midspan strain distribution curve of the top plate at the spigot ends

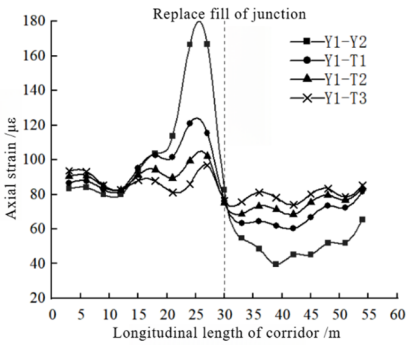

Fig 8c. Midspan strain distribution curve of the bottom plate at the bell ends

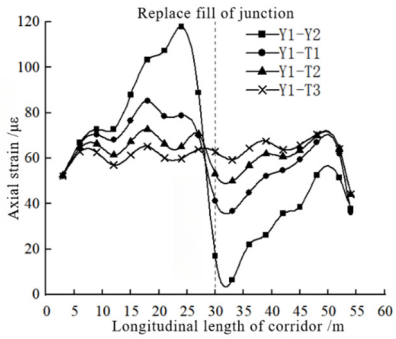

Fig 8d. Midspan strain distribution curve of the bottom plate at the spigot ends

Upon analyzing Figure 8, it is evident that the maximum mid-span strain of the bottom plate at the bell end surpasses the maximum mid-span strain of the top plate by 73%, whereas at the spigot end, it surpasses by 45%. The above research data suggest that the mid-span deformation of the bottom plate is higher than that of the top plate at the same gallery joint. The difference in longitudinal foundation stiffness at the same fill height is directly proportional to the rate of the alteration in the strain curve of the pipe gallery at the replacement junction. These are concretely manifested as the difference in longitudinal foundation stiffness increases, the midspan strain on the top plate at the joint of the replacement section and the bottom plate at the joint of the original soil section increases. Conversely, the midspan strain on the top plate of the original soil section and the bottom plate of the replacement section decreases as the difference in longitudinal foundation stiffness decreases. And the maximum mid-span deformation of the bottom plate is observed to occur at the interface of the two pipe galleries on the left side of the replacement junction, while the maximum mid-span deformation of the top plate is located at the interface of the two to three pipe galleries on the right side of the replacement junction.

Based on a comparison of Figure 8(a), 8(b), 8(c), and 8(d), it can be observed that the mid-span deformation of the top plate at the bell end is about 18% greater than that at the spigot end. Similarly, the mid-span deformation of the bottom plate at the bell end is approximately 42% greater than that at the spigot end. The results show that, for the same joint, the deformation distribution at the inner midspan of the bell and spigot ends is almost identical. However, the inner midspan deformation of the bell end is greater than that of the spigot end, thus the mid-span of the bottom plate at the bell end is particularly prone to cracking damage, corresponding reinforcement measures should be adopted at the joints for the actual construction.

The findings of this study suggest that longitudinal non-uniform foundations may lead to cracking in the bottom plate of the bell end of the pipe gallery joint, followed by the top plate of the bell end. However, cracking is least likely to occur at the top plate of the spigot end. Additionally, it is noted that there are only four potential hazard zones for cracking at a longitudinal non-uniform foundation stiffness difference ratio of λ=20, and all of them are situated on the replacement soil side.

4.3. Deformation Analysis

4.3.1. Longitudinal Horizontal Opening Displacement Analysis

Figure 9 depicts the longitudinal horizontal opening displacement distribution of the top and bottom plates at the prefabricated corridor joint under different foundation conditions.

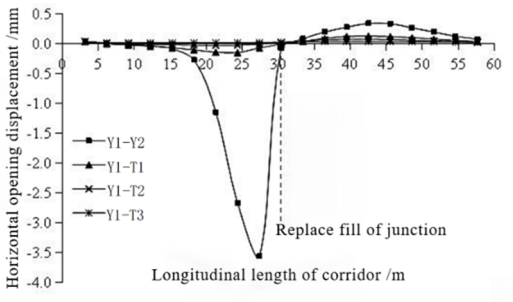

Fig 9a. Midspan strain distribution cloud diagram at the top plate

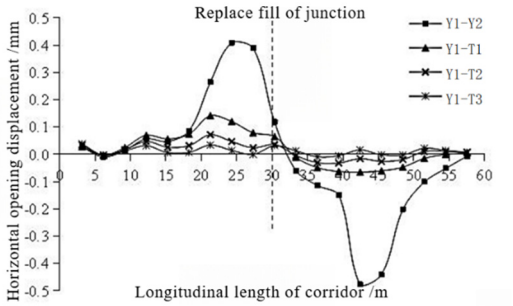

Fig 9b. Midspan strain distribution cloud diagram at the top plate

As can be seen from Figure 9(a) and 9(b), under different foundation conditions, the fluctuation rage of the longitudinal horizontal opening displacement at the interface of the top plate of the corridor on the left side of the replacement junction are in order 0.007~3.561mm, 0.001~0.148mm, 0.003~0.037mm and 0.016~0.039mm; and that of the top plate on the right side are in order 0.077~0.340mm, 0.038~0.128mm,0.030~0.076mm,0.025~0.038mm; and that of the bottom plate on the left side are in order 0.009~0.409mm, 0.003~0.142mm, 0.003~0.072mm, 0.000~0.039mm; and that of the bottom plate on the right side are in order 0.006~0.476mm, 0.001~0.065mm, 0.004~0.032mm, 0.002~0.023mm.

The results indicate that there are significant differences in longitudinal horizontal opening displacement at different joint locations of the pipe gallery under longitudinal uneven foundation stiffness differences. This shows concretely that the probability of cracking occurrence is higher at the top plate of the pipe gallery in the native soil section and the bottom plate of the pipe gallery on the replacement side. In addition, the results indicate that the probability of cracking occurs directly proportional to the magnitude of the difference in longitudinal uneven foundation stiffness. It shows that under the longitudinal uneven foundation differences, the longitudinal horizontal opening displacement at the interface at different locations varies significantly, the inter-sectional cracks are more likely to occur in the top plate of the pipe gallery on the left side of the replacement junction(the side with higher foundation stiffness) and the bottom plate of the pipe gallery on the right side of the replacement junction(the side with less foundation stiffness), and overall the longitudinal horizontal opening displacement increases with the increase of the longitudinal uneven foundation differences, the displacement of the longitudinal horizontal opening of the top plate to the left of the replacement junction, that is at the interface of the pipe gallery on rocky foundations, is most affected by the variation of the longitudinal foundation difference, under the Y1-Y2, the maximum longitudinal horizontal opening displacement on the left side of replacement junction amounts to 3.95mm, which may cause serious water leakage.

When the longitudinal foundation difference is large, the maximum longitudinal horizontal opening displacement of the pipe gallery located in the native soil section occurs at the

top plate of the joint, which is a pipe gallery section away from the replacement junction. Similarly, the pipe gallery on the replacement side exhibits maximum longitudinal horizontal opening displacement at the bottom plate of the joint, which is four sections of pipe galleries away from the replacement junction. When slight differences in longitudinal foundation stiffness occur, compared to the above, the position of the maximum longitudinal horizontal opening displacement of the top plate of the pipe gallery located in the native soil section shifts to the left, approximately 3 to 4 pipe galleries away from the replacement junction. While on the replacement side, the position of maximum longitudinal horizontal opening displacement at the bottom plate of the pipe gallery remains relatively stable.

The results show that with the increase of the difference in the longitudinal stiffness of the foundation, the position of the maximum horizontal opening displacement of the top plate of the pipe gallery located in the native soil section or the side with higher foundation stiffness shifts towards the replacement junction. This phenomenon is substantially influenced by differences in foundation stiffness. In contrast, the maximum horizontal opening displacement position of the bottom plate of the pipe gallery on the replacement side or the side with lower foundation stiffness is not affected by foundation differences.

Under Y1-Y2 working conditions, there are 10 and 6 locations, respectively, at the junction of the top and bottom plates, where the longitudinal horizontal opening displacement exceeds 0.2mm. Among them, the joint position of the first pipe gallery on the left side of the replacement junction has a horizontal opening displacement of 3.561mm, which could potentially lead to serious water leakage incidents. Apart from the Y1-Y2, the longitudinal horizontal opening displacement at the joint of the pipe gallery on both sides of the replacement junction is less than 0.2mm, satisfying the current specifications.

4.3.2. The Vertical Settlement Displacement Analysis

Under various foundation conditions, the vertical settlement distribution of the pipe gallery at bell and spigot ends is illustrated in Figure 10.

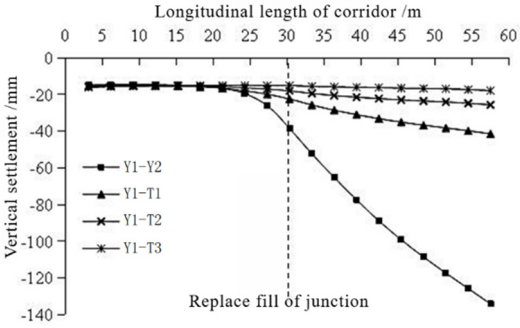

Fig 10a. Longitudinal horizontal opening displacement distribution curve of the top at joints

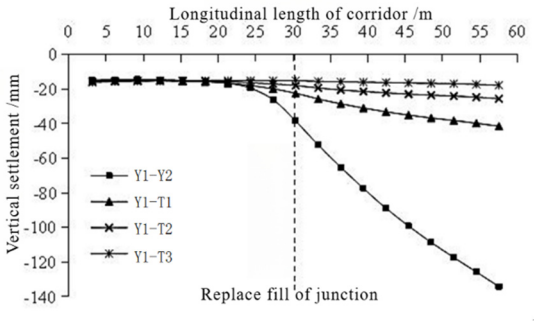

Fig 10b. Longitudinal horizontal opening displacement distribution curve of the bottom at joints

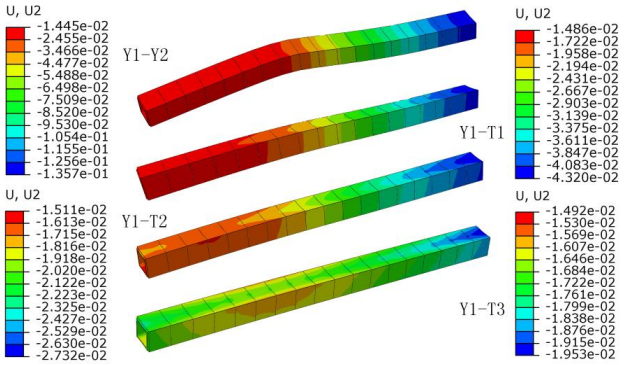

Fig 10c. Vertical displacement cloud of the pipe gallery

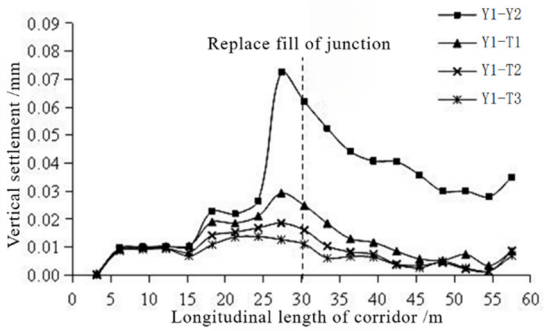

Fig 10d. Differential settlement between bell and socket joints

As Figure 10 demonstrates, the settlement trends at bell and spigot ends in the pipe gallery are essentially the same, with significant differences in settlement present in replacement soil junction. Otherwise, as the longitudinal stiffness differential in the foundation increases, settlement in the replacement foundation side pipe gallery continues to rise. Under Y1-Y2 working conditions, the largest pipe gallery settlement reaches 134.12mm, exceeding the tolerance value of 100mm.

As shown in Figure 10(c), there is an obvious color variation at the replacement soil junction as increasing as the difference in foundation stiffness, indicating a clear different settlement in pipe gallery joints at the replacement soil junction.

As shown in Figure 10(d), under different longitudinal uneven foundation conditions, the largest vertical settlement difference between the bell and spigot ends occurs at the position of the first pipe gallery on the left side of the replacement junction, increasing with the difference in foundation stiffness. The vertical settlement differential range across the bottom plate at the bell and spigot ends of the corridor interface to the left of the replacement soil junction is 0.010-0.073 mm, 0.009-0.026 mm, 0.009-0.019 mm, and 0.009-0.013 mm, respectively. The range to the right of the replacement soil junction is 0.028-0.062 mm, 0.003-0.025 mm, 0.001-0.016 mm, and 0.002-0.011 mm. It indicates that in the case of uneven foundation conditions, the vertical settlement difference between the bell and spigot ends of the

pipe gallery is greater on the side with higher stiffness, and increases with the longitudinal difference in the foundations. Conversely, the settlement difference between the two ends of the corridor is relatively negligible, while the differential settlement caused by soil replacement is considerably higher at the junction, demonstrating a "reducing trend from the site of soil replacement to both sides.

5. Conclusion

Taking a comprehensive urban corridor project in Jishou as the engineering background, the force characteristics of the corridor under different longitudinal uneven foundation conditions are studied under the action of vehicle load, concluded as follow:

1) Under the same uneven longitudinal foundation, axial stresses between the interface joints of the pipe gallery on either side of the replacement junction continuously vary with the height of the fill, forming an "S" shape along the longitudinal axis. At the same fill height, a jointed watertight weak interface with an axial stress of less than 1.5 MPa occurs at the interface of the top plate of the corridor on the left side when the foundation stiffness difference ratio $\lambda \geq 1.25$ and at the interface of the bottom plate of the corridor on the right side when $\lambda \geq 5$.

2) The deformation in the midspan of the bottom plate at the bell end of the pipe gallery is most affected by differences in longitudinal foundation. Maximum deformation occurs at the interface of the 2 to 3 sections of pipe on the right side of the replacement soil junction. The top plate of the bell end is the second largest deformation, while the top plate of the spigot end is the least affected. At the same interface, the deformation at the bell end exceeds that at the spigot end. Overall, deformation increases with greater differences in longitudinal foundation.

3) Under conditions of longitudinal uneven foundation, inter-sectional cracks are more likely to occur at the top plate of the pipe gallery with greater foundation stiffness, and at the bottom plate of the pipe gallery with lower foundation stiffness. The most affected interface is at the top plate of the pipe gallery on the original soil foundation. As the difference in longitudinal unevenness in the foundation increases, the maximum longitudinal horizontal opening displacement position of the top plate of the pipe gallery on the original soil foundation gradually moves closer to the junction with the replacement soil, while the bottom plate of the pipe gallery on the replacement soil foundation remains essentially unchanged.

4) Under the conditions of uneven longitudinal foundation, the settlement trends at the bell and spigot ends of the pipe gallery are basically the same. The vertical settlement difference between the bell and spigot ends of the pipe gallery is greater on the side with higher stiffness, and increases with the longitudinal difference in the foundations. The maximum vertical differential settlement between the bell and spigot ends of the pipe gallery is located at the interface of the first section of the pipe gallery on the left side of the replacement junction, demonstrating a 'reducing trend from the junction of soil replacement to both sides.'

5) This paper aims to investigate the mechanical properties of pipe gallery joints under uneven settlement. However, it is noted that the load-bearing characteristics of joints may vary after failure. Further research can be carried out on crack and seepage characteristics, deformation patterns of the surrounding soil, and measures taken to reinforce the structure once the gallery is compromised.

Data Availability Statements

All data, models, and code generated or used during the study appear in the submitted article.

References

[1] XIE Shengxing. The application of shallow soft foundation replacement process in the construction of urban integrated pipe gallery[J]. Engineering Technology: 00231-00231.

[2] KOU Zhentao, YANG Xu, LIU Kui. Analysis of Failure Modes and Mechanism of Building Foundations in Semi-filling and Semi-excavating Sites of Loess Area[J]. Journal of Water Resources and Architectural Engineering, 2018, 16(03): 175-181.

[3] WANG Hong. Numerical simulation of rock stability in half-rock and half-earth tunnels[C].Underground Traffic Engineering and Engineering Safety--Proceedings of China's 5th International Symposium on Tunnelling, 2011: 626-632.

[4] SHEN Wenming, TANG Xiaowu, BIAN Xuecheng et al.Study on the Longitudinal Mechanical Model of Buried Culvert During Foundation Differential Settlement [J] College of Architecture and Engineering, 2010,40(10):82-85.

[5] ZHANG Xiaobin, LE Jinchao.Calculation of Static Earth Pressure on Retaining Wall of Cut-and-fill Subgrade [J] Journal of Highway and Transportation Research and Development, 2014:31(06):17-22.

[6] YAN Yufeng, HUANG Qiangbin, YANG Xuejun et al.Research on the Deformation and Force Characteristics of Underground Utility Tunnel Crossing Ground Fissure [J] Journal of Engineering Geology, 2018:26(05):1203-1210.

[7] QU Jian.Dynamic Research of Utility Tunnel under the Effect of Oblique Incidence of Ground Motions[D]. Harbin Institute of Technology, 2017.

[8] LI Haizhen, FENG Xin, ZHAO, Lin. Failure analysis of a buried large-diameter prestressed concrete cylinder pipeline subjected to strike-slip fault displacement[J]. Tunnelling and underground space technology,2022,121(Mar.):104334.1-104334.12.

[9] Yi Z . Construction technologies of anti-seepage treatment for socket-connected-joint[J]. Shanxi Architecture, 2017.

[10] LI Xiangyu, LI Xinyuan, LI Mingyu et al.Study on the Influence of Different Degrees of Leakage on Long-term Settlement of Shield Tunnels[J]. MODERN TUNNELLING TECHNOLOGY,2022,59(05):72-79.

[11] Sonoda Y , Sawada Y , Ono K , et al. Three-dimensional Deformation Behavior for Buried Pipe Joints Subjected to Local Differential Settlement Using Three-direction Strain Measurement[J]. Transportation Infrastructure Geotechnology, 2022:1-22.

[12] BAI Xufeng, ZHANG Jing, SU Xiaoguo.Effects of Soft Soil Foundation with Long-term Differential Settlement on Precast Concrete Utility Tunnel [J] Low Temperature Architecture Technology,2018,40(10):86-87.

[13] MIAO Chenyang, HUANG Qiangbin, Gou Yuxuan et al. Study on the Impact of Shield Tunnel Under-crossing at Ground Fissure Site on Existing Utility Tunnel[J]. Modern Tunneling Technology,2022,59(03):155-165+171.

[14] WEI Gang, ZHU Xinguang, SU Qinwei. Research on the calculation method and distribution of vertical uneven settlement in immersed tube tunnels[J]. Modern Tunneling Technology,2013, 050(006):58-65.

[15] SHAO Junjiang.Research on Settlement Prediction and Control of Immersed Tunnel [D] Tongji University,2003.

[16] Grantz W C . Immersed tunnel settlements Part 1: Nature of settlements [J]. Tunnelling and Underground Space Technology, 2001, 16(3):195-201.

[17] Grantz W C .Immersed tunnel settlements part 2: Case histories [J]. Tunnelling & Underground Space Technology Incorporating Trenchless Technology Research, 2001, 16 (3): 203-210.

[18] XU Jian, XIE Zhongqiu, WU Jinglong.Study on the deformation characteristics of integrated pipe gallery under vehicle load[J]. Building Structure, 2019, 49(S1): 845-849.

[19] Tang L , Quan Y , Zhu Y , et al. Application of improved calculation method considering the vehicle loads in branch utility tunnel[J]. Geotechnical and Geological Engineering, 2019, 37(1):251-266.

[20] Shi, X.M. & Cai, C.S.. Simulation of dynamic effects of vehicles on pavement using a 3D interaction model[J]. Journal of Transportation Engineering, 2009,135(10):736-744.

[21] QIU Minyu, YU Yanan.Analysis of influence depth for roads induced by vehicle load.[J] Rock and Soil Mechanics, 2010:31 (06): 1822-1826.

[22] Ministry of Housing and Urban-Rural Development of the People's Republic of China.GB50838-2015 Technical specifications for urban integrated pipe corridor projects [S]. Beijing China Planning Publishing House,2015.